



$$\text{Re } s_i < a < 0$$

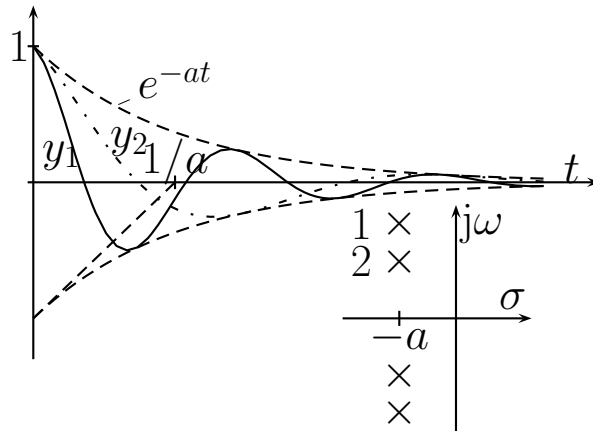


Figure 3.1. Two solution terms with the same negative real part  $\sigma = -a$  of the eigenvalues.

$y_2$  has better damping

$$\begin{aligned} p_i(s) &= (s - \sigma_i - j\omega_i)(s - \sigma_i + j\omega_i) \\ &= s^2 - 2\sigma_i s + \sigma_i^2 + \omega_i^2 = s^2 + 2D\omega_0 s + \omega_0^2. \end{aligned}$$

**Natural frequency**

$$\omega_0 = \sqrt{\sigma_i^2 + \omega_i^2}$$

**Damping**

$$D = -\sigma_i/\omega_0$$

Real and imaginary part of EV

$$\sigma_i = -D\omega_0, \quad \omega_i = \omega_0\sqrt{1 - D^2}$$

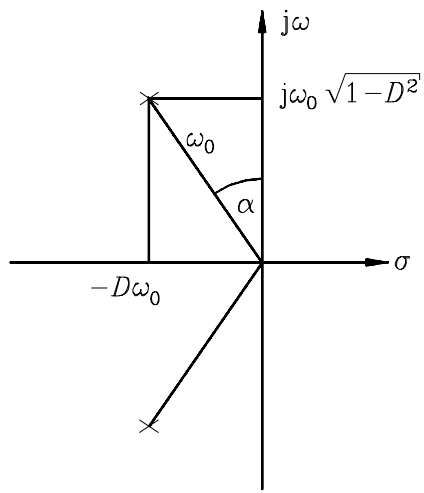


Figure 3.2. Natural frequency  $\omega_0$  and damping  $D$  of a complex conjugate pair of poles.

$$D = \sin \alpha. \quad (3.1.1)$$

## Time domain

$$y_i(t) = A e^{-D\omega_0 t} \cos\left(\sqrt{1 - D^2}\omega_0 t + \varphi\right) \quad \text{for } |D| < 1 \quad (3.1.2)$$

$\omega_0 t =$  scaled time

Amplitude  $A$  and angle  $\varphi$  depend on initial conditions

Step response of

$$g(s) = \frac{1}{1 + 2Ds/\omega_0 + s^2/\omega_0^2} \quad (3.1.3)$$

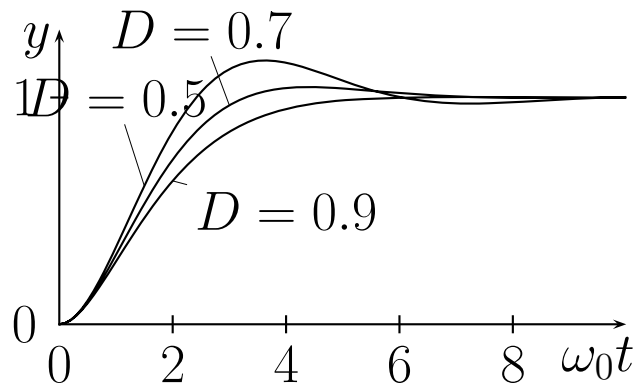


Figure 3.3. Step responses of the system (3.1.3).

For  $D = 1/\sqrt{2} \approx 0.7$       $\alpha = 45^\circ$

maximum overshoot 4,3%

frequency response  $|g(j\omega)|$  has maximum at resonance  
frequency  $\omega_0 = \sqrt{1 - 2D^2}$  for  $D < 1/\sqrt{2}$ .

## Effect of a zero at $s = -b\omega_0$

Step response of

$$g(s) = \frac{(1 + s/(b\omega_0))}{1 + 2Ds/\omega_0 + s^2/\omega_0^2} \quad (3.1.5)$$

$$D = 1/\sqrt{2}$$

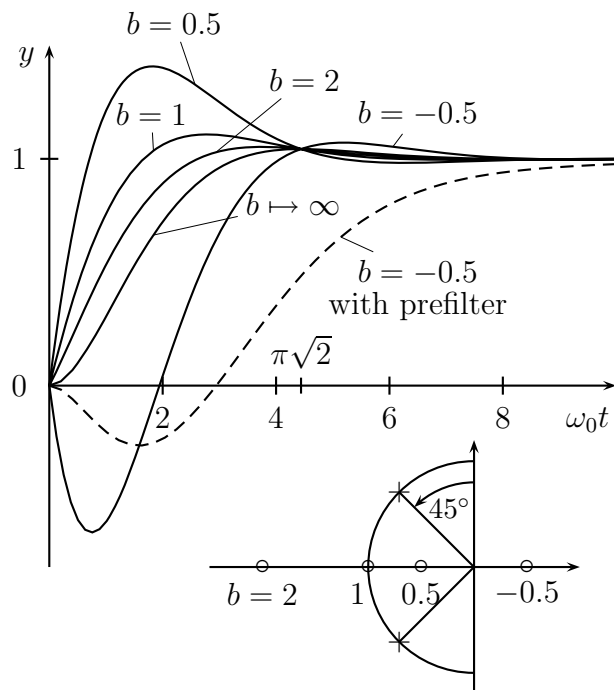


Figure 3.4. Step response of the system (3.1.5) for different zero locations  $b$ .

$b = \infty \rightarrow$  No zero, zero slope at  $t = 0$

$b = 2 \rightarrow$  steep slope at  $t = 0$

$b = 1 \rightarrow$  faster

$b = 0.5 \rightarrow$  40.7% overshoot

cancellation or smaller  $\omega_0$

$b < 0 \rightarrow$  nonminimum phase, step response

starts in negative direction

Reduce undershoot by mirror cancelation

by  $0.5/(s+0.5)$ , slow response

## Effect of a real pole at $s = -a\omega_0$

Step response of

$$g(s) = \frac{1}{(1 + 2Ds/\omega_0 + s^2/\omega_0^2)(1 + s/(a\omega_0))} \quad (3.1.7)$$

Similar effect as increased damping therefore  **$D = 0.5$**

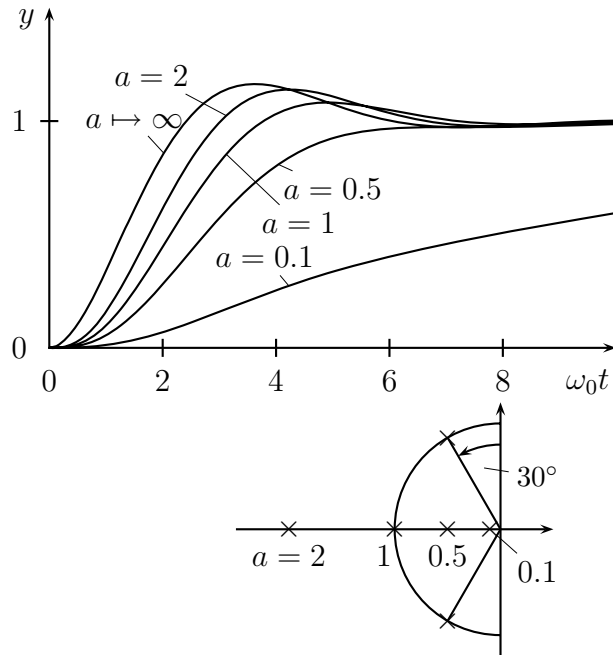


Figure 3.5. Influence of a pole at  $s = -a$  on the step response.

$a = \infty$	No pole, 15.5 % overshoot
$a = 2$	8.1 % overshoot
$a = 1$	Butterworth pole pattern
$a = 0.5$	no overshoot
$a \rightarrow 0$	sluggish response by dominating real pole
$a < 0$	unstable

## Relations between step responses and eigenvalues

- 1) Oscillatory response with period  $T$  caused by a complex pole pair in a distance  $\omega_0 = 2\pi/T$  from the origin

Improve damping of this pole pair or shift a real pole to  $s = -2\pi/T$  (Butterworth configuration).

- 2) Nonoscillatory overshoot caused by a zero closer to the origin than the dominant pole pair.

Reduce natural frequency of dominant pole pair.  
Cancellation? May cause large  $u$ .

- 3) Sluggish response caused by a dominant real pole close to the origin.

Shift this pole to the left.

#### 4) High frequency ripple

Reduce bandwidth (e.g. reduce  $\omega_0$ , use controller with difference degree one).

In sampled-data systems use anti-aliasing filter before the sampler.

#### 5) Initial response in wrong direction caused by non-minimum phase zeros.

Cannot be removed but alleviated by mirror cancellation in LHP.

#### 6) Excessive initial peak in actuator signal caused by non-dominant complex poles.

Use low pass prefilter.

For SISO systems

- 7) Shifting poles close to the zeros causes high gains (root locus)
- 8) If open loop has relative degree  $\rho_0 \geq 2$  then “center of gravity” of EV (plant + compensator) cannot be shifted.

$$p(s) = \underbrace{a_0 + \dots + a_{m-2}s^{m-2}}_{\text{changed by compensator zeros and gain}} + a_{m-1}s^{m-1} + s^m$$

changed by

compensator

zeros and gain

$$p(s) = \prod_{i=1}^m (s - s_i) \rightarrow a_{m-1} = - \sum_{i=1}^m s_i \quad (CG)$$

Choose compensator poles sufficiently far left.

- 9) Avoid pole-zero cancellations outside  $\Gamma$ , otherwise not internally  $\Gamma$ -stable.

## Root Sets

Crane  $m_C = 1000$

$m_L \in [1000; 2000]$ ,  $\ell \in [8; 16]$

“Nominal case”  $m_L = 1500$ ,  $\ell = 12$

the output feedback controller

$$u = -K [500 \quad 2191 \quad -4299 \quad 0] \mathbf{x}, \quad K = 1$$

shifts the eigenvalues to  $s_{1,2} = -0.59 \pm 1.06j$ ,  
 $s_{3,4} = -0.51 \pm 0.16j$ .

Pole placement yields unique feedback gains. Uniqueness means: For same eigenvalues and different  $m_L, \ell$  different feedback required. Alternative: let eigenvalues vary in a limited neighborhood of  $s_{1,2}$ .

Analysis by root set for a grid on  $Q$ .

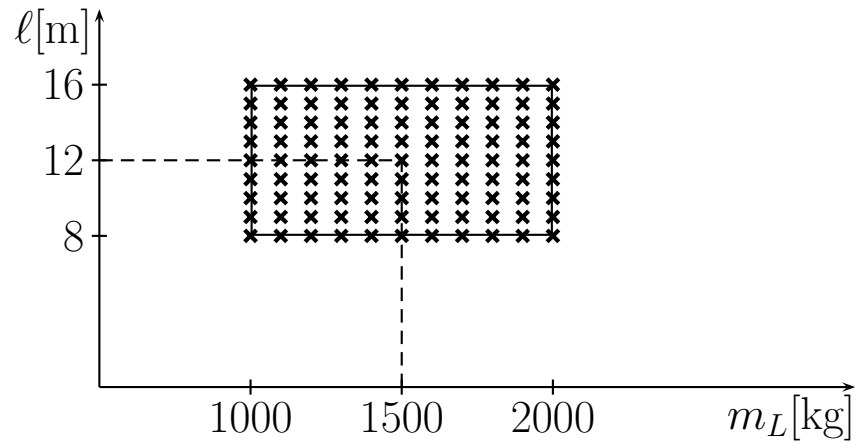


Figure 3.6. An  $11 \times 9$  grid over the operating domain  $Q$ .

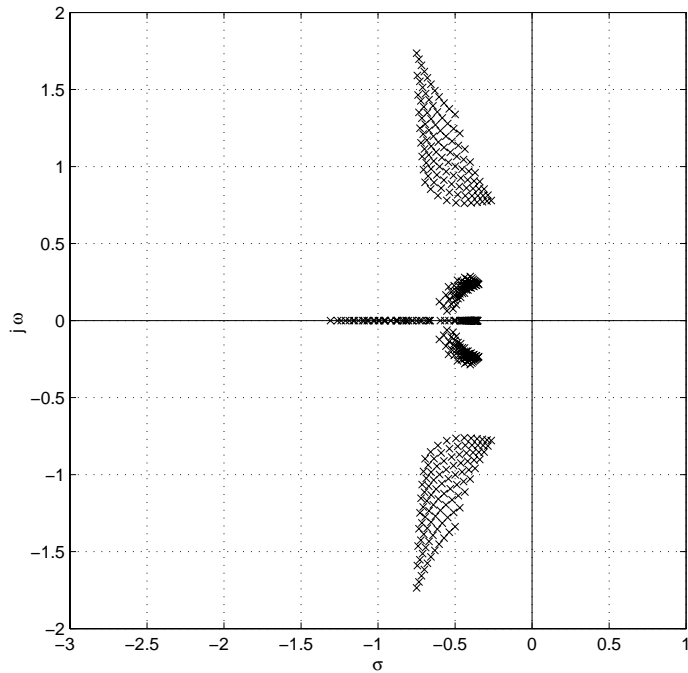


Figure 3.7. Root set for the grid points of Figure 3.6.

## $\Gamma$ -stability

Choose the left branch of the hyperbola  $\omega^2 = 4\sigma^2 - 0.25$  as the  $\Gamma$ -stability boundary. It passes through the nominal poles at  $s_{1,2} = -0.59 \pm 1.06j$ . How to modify the controller such that the root set becomes  $\Gamma$ -stable?

Trial and error is time consuming, not systematic.

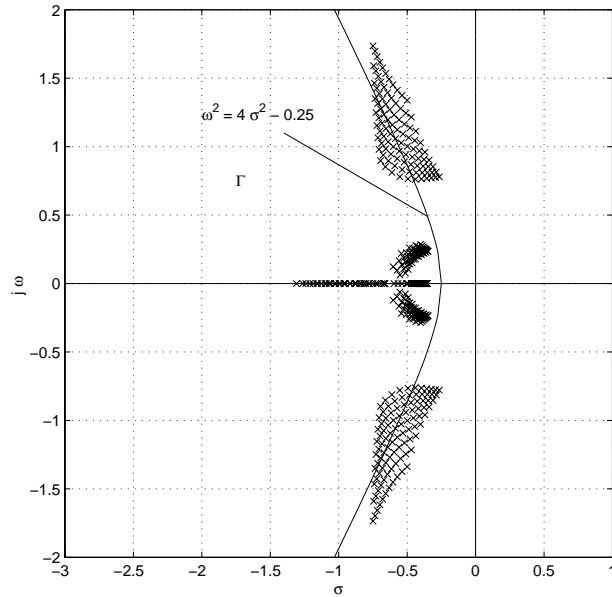


Figure 3.9.  $\Gamma$ -stability specified by a hyperbola.

## Parameter space approach

Derivation of mapping equations see Chapter 4.

Consider the vertex  $m_L = 1000$ ,  $\ell = 8$  of the operating domain  $Q$  and the controller

$$u = -[500 \ k_2 \ k_3 \ 0] \mathbf{x}. \quad (3.2.2)$$

The boundary  $\omega^2 = 4\sigma^2 - 0.25$  with parameter  $\sigma$  is mapped to the  $(k_2, k_3)$ -plane in Fig.3.10.

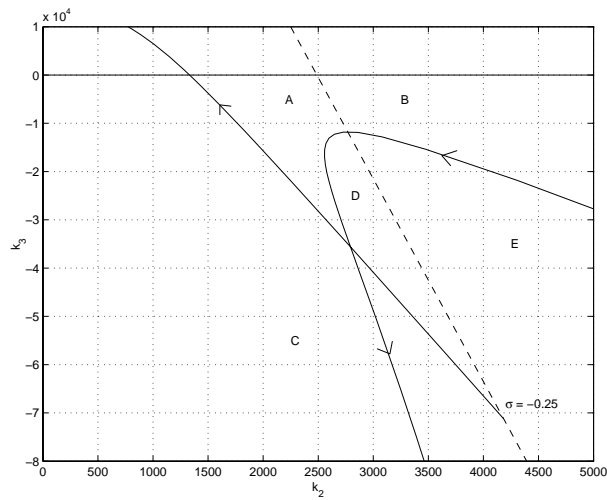


Figure 3.10. On the boundary lines there are closed-loop eigenvalues on the hyperbola.

## Reduce to active boundaries

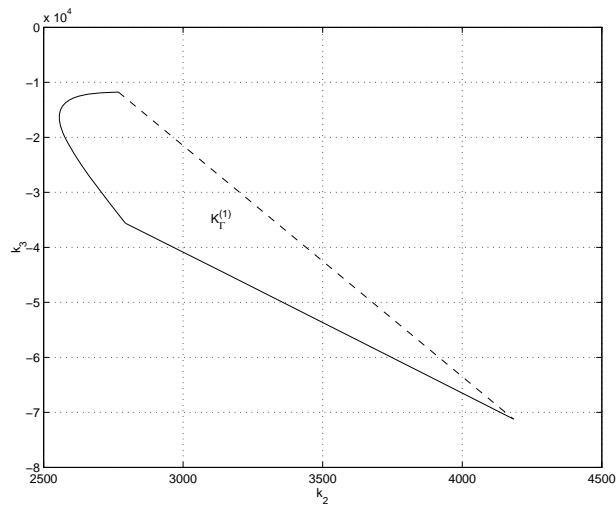


Figure 3.11. Active boundaries from Fig.3.10.

Same for other 3 vertices of  $Q$

Intersection = Set of all simultaneous  $\Gamma$ -stabilizers for four vertices of  $Q$ .

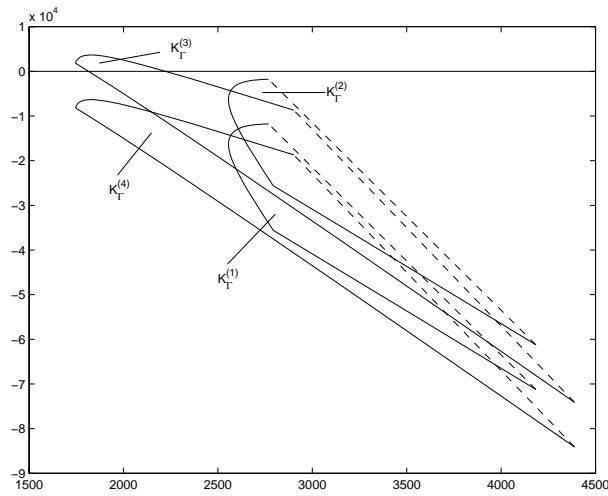


Figure 3.13.  $\Gamma$ -stabilization of the four vertices of  $Q$ .

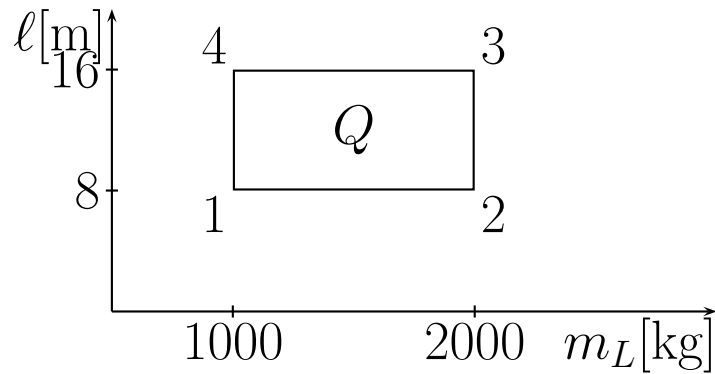


Figure 3.12. The operating domain and four representatives.

Only operating conditions 2 and 4 contribute to boundary.

Choose a centrally located controller.

$$u = -[500 \quad 2639 \quad -15255 \quad 0] \mathbf{x} \quad (3.2.4)$$

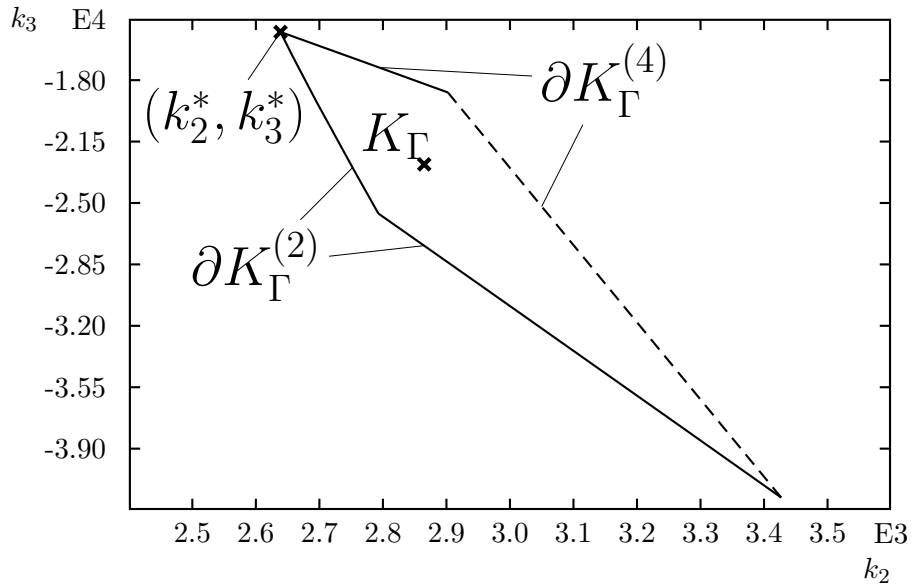


Figure 3.14. Intersection of the four regions of Fig.3.13.

Fix controller

$$u = -[500 \quad 2639 \quad -15255 \quad 0] \mathbf{x} \quad (3.2.4)$$

Map  $\partial\Gamma$  into  $(m_L, \ell)$ plane

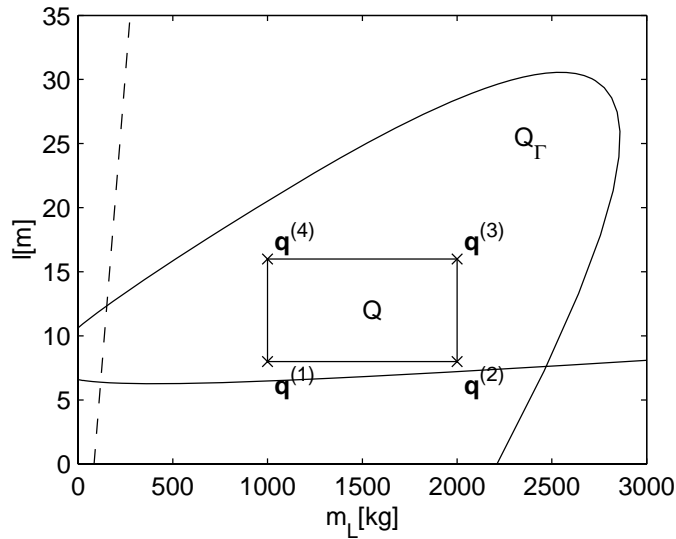


Figure 3.16. Robustness analysis in the  $(m_L, \ell)$ -plane.

Entire  $Q$ -box is stable

For comparison root set

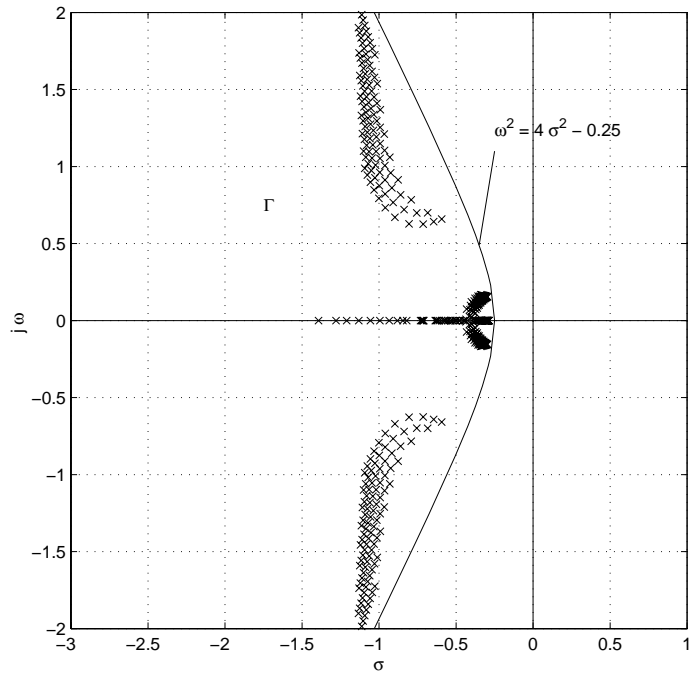


Figure 3.15. Root set for the controller 3.2.4.

# Physical meaning of closed-loop poles

In a one-shot pole placement the idea of relating the closed-loop poles to the open-loop poles is lost.

Crane

$$u = -K [500 \quad 2191 \quad -4299 \quad 0] \mathbf{x}, \quad K = 1$$

So far  $K = 1$  now let  $K$  grow from zero to one  
Eigenvalue tracing

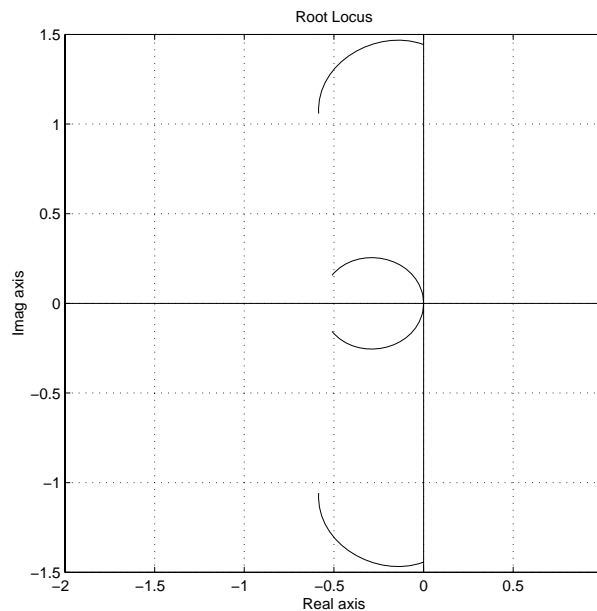


Figure 3.18. Eigenvalue tracing for continuously growing loop gain.

Pendulum swings with higher frequency than crab.

One-to-one relationship is destroyed by crossing a branching point.

Example

$$u = -K [500 \ 0 \ 15508 \ 0] \mathbf{x} \quad (3.3.1)$$

For  $K = 1$  double imaginary roots at  $\pm j 0.803$ .

For  $K > 1$  no distinction between crab and pendulum eigenvalues possible.

Branching point

$$p(s) = 0 \quad \text{and} \quad (3.3.2)$$

$$\frac{dp(s)}{ds} = 0.$$

For design transparency avoid crossing a branching point.

## Existence of Robust Controllers

For a plant with nominal parameter values a necessary and sufficient condition for  $\Gamma$ -stabilization, is that all EV outside  $\Gamma$  must be controllable and observable.

Condition does not carry over to simultaneous stabilization of a plant family.

*Example* Hurwitz stabilization of the finite plant family

$$g^{(1)}(s) = \frac{1}{s-1}, \quad g^{(2)}(s) = \frac{-1}{s-1} \quad (3.4.1)$$

The unstable pole at  $s = 1$  is controllable and observable. The two plants cannot be simultaneously stabilized by a common linear controller.

Proportional feedback:

$g^{(1)}(s)$  stabilized by  $k > 1$

$g^{(2)}(s)$  stabilized by  $k < -1$

Dynamic compensator:

Necessary stability conditions  $a_i > 0$  cannot be simultaneously satisfied (see book).

Interpolation  $a/(s-1)$ ,  $a \in [-1; 1]$  crosses non-controllable value  $a = 0$ .

**Necessary and sufficient conditions for simultaneous  $\Gamma$ -stabilization of a plant family are not known.**

# Representation planes

- a) design: intersection in  $(k_2, k_3)$ -plane
- b) analysis in  $(m_L, \ell)$ -plane
- c) **Gain scheduling** in  $(\ell, k_3)$ -plane for measured  $\ell$

## Crane

$m_C = 1000, m_L = 1500, k_1 = 500, k_2 = 2865, k_3 = -22800$ , find a gain-scheduling controller  $k_4(\ell)$  that meets the  $\Gamma$ -specification (roots left of  $\omega^2 = 4\sigma^2 - 0.25$ ) also at very small rope length  $\ell$ .

Map  $\Gamma$ -boundary to  $(\ell, k_4)$ -plane for  $m_L = 1000$  and  $m_L = 2000$ .

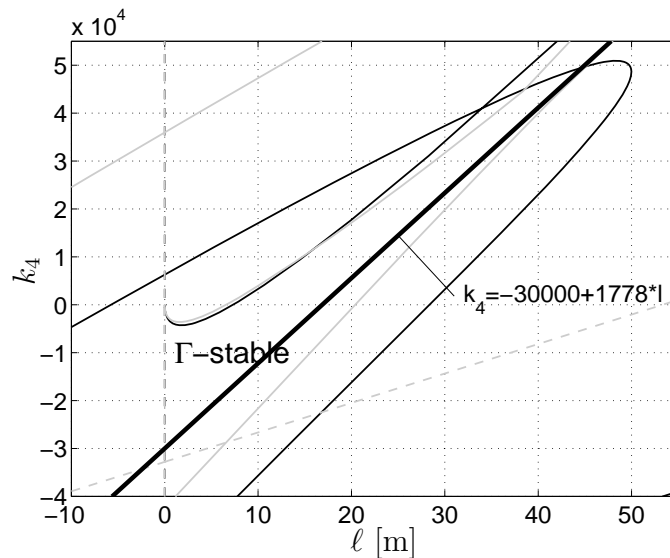


Figure 3.19. Gain scheduling of  $k_4(\ell)$  for the crane

Choose gain-scheduling  $k_4(\ell) = -30000 + 1778 \ell$ .

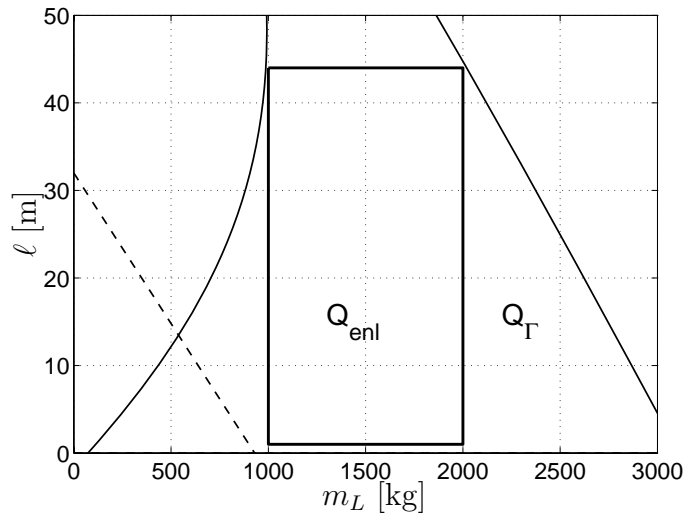


Figure 3.20. An enlarged operating domain (in terms of  $\ell$ ) becomes feasible by gain-scheduling according to Figure 3.19

For comparison: without gain scheduling

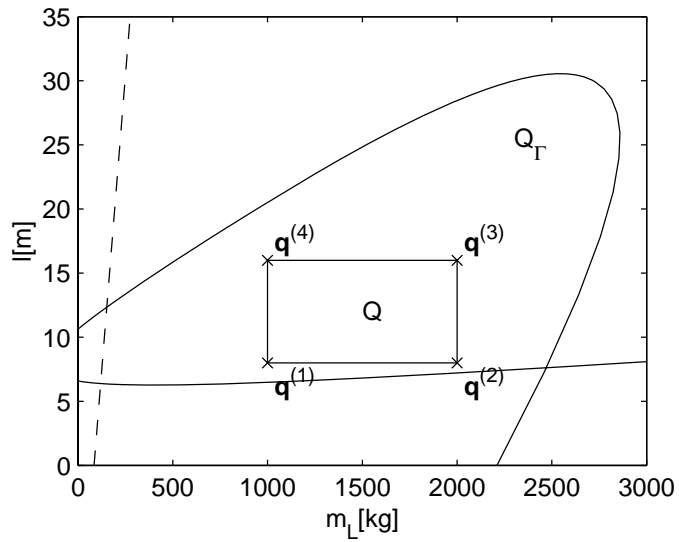


Figure 3.16. Robustness analysis in the  $(m_L, \ell)$ -plane

# From Parameter Plane to Parameter Space

Parameter plane for two parameters yields intuitive figures.

Third parameter may be gridded

Design

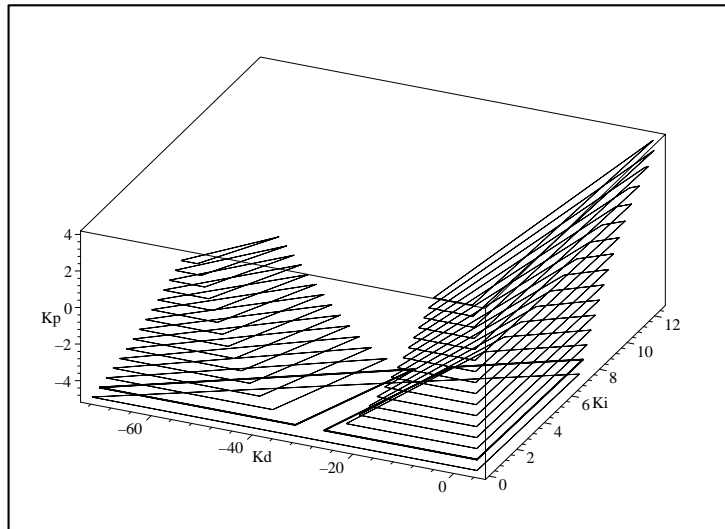


Figure 2.10. The set of all stabilizing PID controllers.

## Analysis

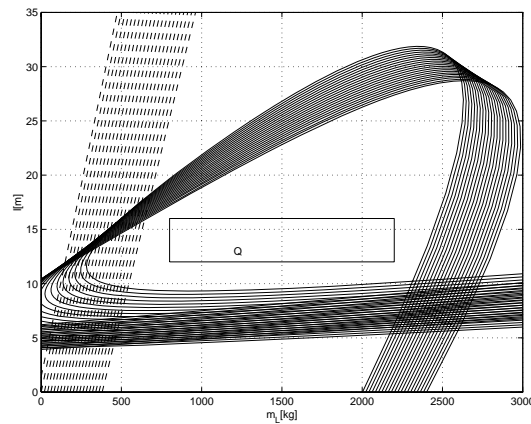


Figure 4.9.  $\Gamma$ -stability boundaries by gridding  $m_C$  which enters together with  $\ell$  bilinearly into the characteristic polynomial.

Crane with gridded crab mass  $m_C$ .

Also for a fourth or fifth gridded parameter.